Stem Cells Translational Medicine, 2023, **12**, 811–824
https://doi.org/10.1093/stcltm/szad064
Advance access publication 29 September 2023
Original Research

Early Postnatal Expression of Tgfβ-1 and Fgf-2 Correlates With Regenerative Functions of Unrestricted Somatic Stem Cell Infusion After Rabbit GMH-IVH

Dina A. Finkel[1], Ana Malfa[1], Yanling Liao[2], Deepti Purohit[1], Furong Hu[2], Davud Sulaymankhil[3], Sai Abhishek Narra[4], Karen Hussein[1], Selvakumar Subbian[5,‡], Mitchell S. Cairo[2,6,‡], Govindaiah Vinukonda[*,2,4,‡], Edmund F. La Gamma[*,1,2,7]

[1]Department of Pediatrics, The Regional Neonatal Center, Maria Fareri Children's Hospital at Westchester Medical Center, Division of Newborn Medicine, New York Medical College, Valhalla, NY, USA
[2]Department of Pediatrics, New York Medical College, Valhalla, NY, USA
[3]Department of Chemical Engineering, Cooper Union, NYC, NY, USA
[4]Cell Biology & Anatomy, New York Medical College, Valhalla, NY, USA
[5]Department of Medicine, Public Health Research Institute, New Jersey Medical School, Rutgers, The State University of Newark, NJ, USA
[6]Departments of Medicine, Pathology, Microbiology & Immunology, New York Medical College, Valhalla, NY, USA
[7]Department of Biochemistry and Molecular Biology, New York Medical College, NY, USA

[*]Corresponding author: Govindaiah Vinukonda, The Regional NICU, Division of Newborn Medicine, Maria Fareri Children's Hospital at Westchester Medical Center, New York Medical College, 100 Woods Road, Valhalla, New York 10595, USA. Tel: +1 914 493 8558; Email: g_vinukonda@nymc.edu; or, and Edmund F. La Gamma, MD, FAAP, The Regional NICU, Division of Newborn Medicine, Maria Fareri Children's Hospital at Westchester Medical Center, New York Medical College, 100 Woods Road, Valhalla, New York 10595, USA. Email: Edmund_LaGamma@nymc.edu.
‡Co-senior authors.

Abstract

Intraventricular hemorrhage (IVH) is a severe complication of preterm birth associated with white matter injury (WMI) and reduced neurogenesis. IVH commonly arises from the germinal matrix, a highly cellular, transient structure, where all precursor cells are born, proliferate, and migrate during brain development. IVH leads to reduced progenitor cell proliferation and maturation and contributes to WMI. Interruption of oligodendrocyte lineage (OL) proliferation and maturation after IVH will prevent myelination. We evaluated whether unrestricted somatic stem cells (USSCs) could recover OL lineage, as USSC release multiple relevant growth factors and cytokines. The effects of USSC infusion at 24 hours after IVH were assessed in the periventricular zone by analysis of OL lineage-specific progression (PDGFR+, OLIG2+, NKX2.2+ with Ki67), and this was correlated with growth factors TGFβ1, FGF2 expression. The early OL cell lineage by immunofluorescence and cell density quantitation showed significant reduction after IVH ($P < .05$ both PDGFR+, OLIG2+ at day 3); with significant recovery after injection of USSCs ($P < .05$ both PDGFR+, OLIG2+ at day 3). CSF protein and tissue mRNA levels of TGFβ1 were reduced by IVH and recovered after USSC ($P < .05$ for all changes). FGF2 showed an increased mRNA after USSC on day3 ($P < .05$). Cell cyclin genes were unaffected except for the cycle inhibitor $P27^{Kip1}$ which increased after IVH but returned to normal after USSC on day 3. Our findings demonstrated a plausible mechanism through which USSCs can aid in developmental myelination by recovery of OL proliferation and maturation along with correlative changes in growth factors during brain development.

Key words: unrestricted somatic stem cells; intraventricular hemorrhage; germinal matrix; subventricular zone; oligodendrocyte; corona radiata; corpus callosum; cerebral palsy; intraventricular hemorrhage; white matter injury; TGFβ-1; FGF-2; premature newborns.

Received: 12 April 2023; Accepted: 9 September 2023.

Graphical Abstract

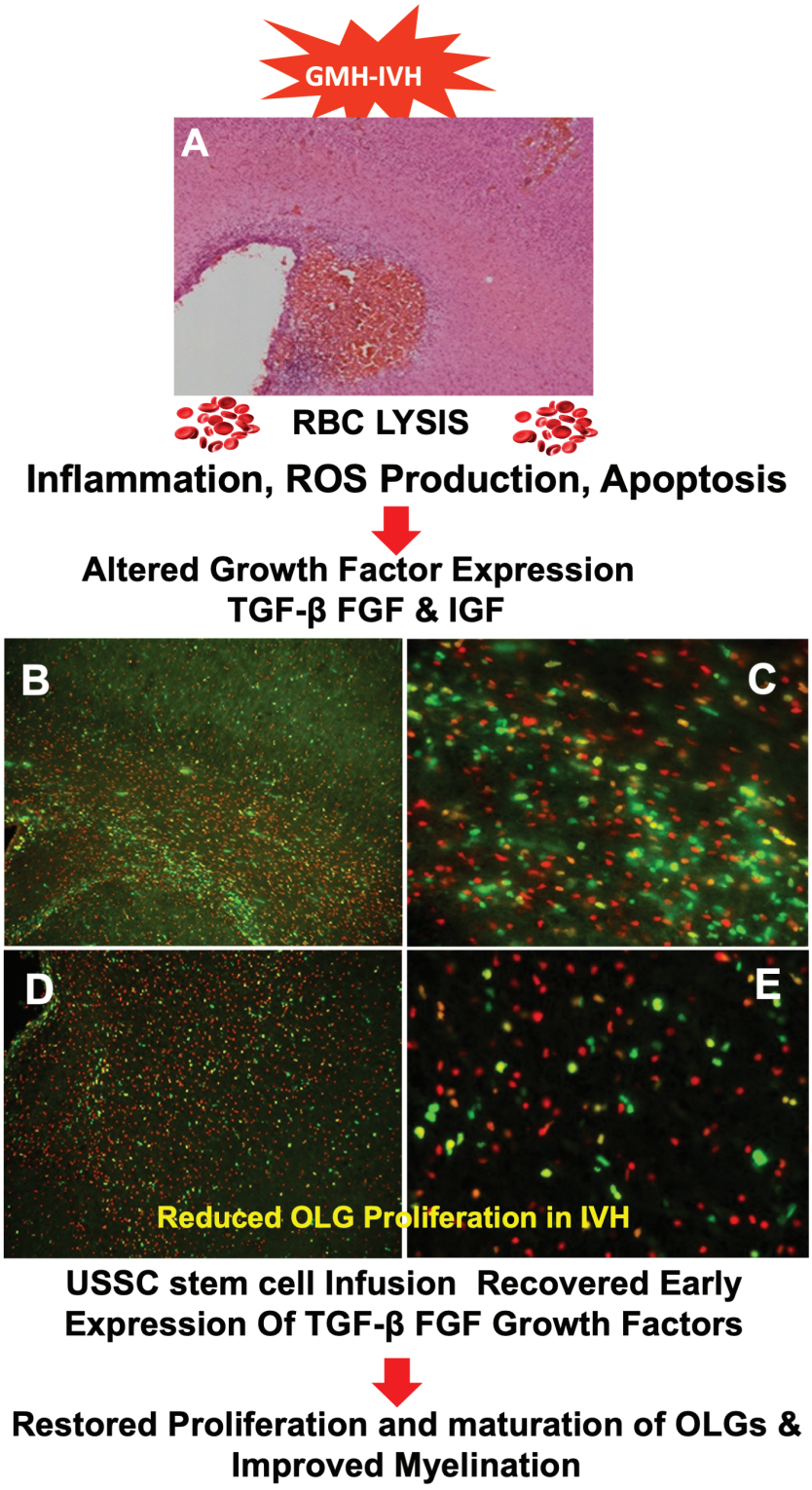

Significance Statement

Although IVH pathologies and therapeutic attempts have been investigated for decades, currently, there is no definitive or universally successful therapy. Our study showed that USSCs administered within 24 hours after IVH provided cell regenerative functions associated with reversal of impaired OL proliferation and maturation corresponding with improved myelination. USSCs also enhanced relevant growth factors and a cell cycle gene that participates in OL proliferation and maturation. Taken together, these findings support the possibility for evaluation of USSCs in translational studies as treatment for IVH in human neonatal clinical trials.

Introduction

Intraventricular hemorrhage (IVH) is a devastating complication of premature birth that most commonly arises from the sub-ependymal germinal matrix (GM) with subsequent rupture into the lateral ventricles as well as into the parenchyma of the subventricular zone (SVZ) and ventricular zone (VZ). The GM is an extremely cellular, highly vascularized transient structure where neuronal and glial precursor cells originate and migrate radially during embryonic and postnatal brain development. A germinal matrix-intraventricular hemorrhage (IVH) is followed by reactive gliosis and an associated decrease in proliferation of oligodendrocyte precursor cells (OPC) and a decrease in oligodendrocyte (OL) differentiation into mature OLs.[1,2] Collectively, this results in reduced neurogenesis, severe white matter injury (WMI) and serious clinical sequelae including hydrocephalus, cerebral palsy, and intellectual disability.[3,4]

Central nervous system progenitor cell proliferation, migration, and maturation are fundamental developmental processes that serve an essential role in normal and pathological brain recovery. The SVZ is the primary source of precursors of astroglia cells[5] beginning before birth as oligodendrocyte precursor cells (OPC), and continuing through adulthood by continuously differentiating into mature myelinating oligodendrocytes.[6-10] The process is complex and involves intrinsic signals from the GM and extrinsic signals from meninges, blood vessels, and cerebrospinal fluid.[11] Each developmental stage can be identified in the sub-ventricular zone (SVZ), corpus callosum (CC), and corona radiata (CR) using various phenotypic markers of: (1) *early* oligodendrocyte precursor cells (PDGFRα$^+$) followed by (2) *late* oligodendrocyte precursor cells (Olig2$^+$, Nkx2.2$^-$) then (3) *immature* myelinating oligodendrocytes (Oligo2$^+$ Nkx2.2$^+$ MBP–, CC, and CR) and finally (4) mature myelinating oligodendrocytes (Olig2$^+$ NKx2.2$^+$ MBP$^+$, CC, and CR).

In cell culture experiments, transforming growth factor beta-1 (TGFβ1), fibroblast growth factor-2 (FGF2), and insulin-like growth factor-1 (IGF1) are important mediators of proliferation and differentiation of the OL lineage.[12-18] Specifically, FGF2 promotes proliferation of neuronal *progenitor* cells and oligodendrocyte *precursor* cells in the developing brain through FGF receptors using a Sonic hedgehog-dependent pathway.[11,18-22] In contrast, TGFβ1 infusion in animals augmented axonal regeneration by inducing cell proliferation and cell cycle entry/exit of *mature* oligodendrocytes during myelination.[18,23,24]

TGFβ1, FGF2, and IGF contribute to progenitor cell proliferation and maturation through cyclin genes by activation of cyclin-dependent kinase (CDK) enzymes.[19,20,24,25] The cyclin dependent kinase (CDK) interacting protein, (CIP)/kinase inhibitory protein (KIP), and INK4 family of proteins are *negative* regulators of the G1/S cell cycle phase transition. CIP/KIP is a protein complex consisting of 3 proteins: p21$^{Cip1/Waf1}$, p27^{Kip1}, and p57^{Kip2}. Cleavage of p21$^{Cip1/Waf1}$ into p21^{Cip1} (CDKN1A) and p18^{Ink} (CDNK2C) are also implicated in regulation of OL cell growth and cell responses to DNA damage. The protein p21^{Cip1} (CDKN1A) protects against apoptosis and is essential to foster cell survival. The protein p27^{Kip1} (CDKN1B) is a G1 arrest and negative regulator of the proliferative activation of the oligodendrocyte lineage both in vitro and in vivo.[26-28] Taken together, changes in expression of these cell cycle genes can be used to characterize stages of cell division or arrest during progression of oligodendrocyte lineage and myelination after injury or in response to interventions.

"Living therapy" using exogenously administered stem cells offers great hope for the treatment of IVH as these cells migrate to areas of injury, survive long enough to alter the extracellular microenvironment, and promote recovery without fully engrafting the organ.[29-33] Kogler et al and our group characterized human cord blood (hCB)-derived unrestricted somatic stem cells (USSCs) and studied their proliferation, expansion, gene and cytokine expression, epigenetic modification, and lineage differentiation in various models.[34-37] We were the first to demonstrate that USSCs migrate to the site of injury, suppress inflammation, reduce hydrocephalus, improve myelination as well as neurodevelopmental outcomes in a premature rabbit pup model of IVH.[38,39] Other investigators show that USSCs induce significant axonal regrowth and effectively improve long-term functional locomotory and neurobehavioral recovery.[40] Moreover, USSC transplantation promotes tissue sparing, which might contribute to enhanced locomotor and neurobehavioral improvement.

In the present study, we sought to determine whether intracerebroventricularly (ICV) administrated USSCs altered OL lineage-specific densities of proliferating OPCs and maturation of early and late OLs. We examined changes in the levels of key growth factors: TGFβ1, FGF2, and IGF, as they are already known to regulate oligodendrocyte lineage in the developing brain. Downstream effects of these factors involved in regulating cyclin gene expression during proliferation and maturation of OPCs/OLs were used to assess for corroborating evidence of the impact of USSCs on recovery of cell division in the SVZ and PVZ white matter of the developing forebrain.

Methods

Human Cord Blood-Derived Unrestricted Somatic Stem Cells

We used previously isolated USSCs from hCB according to published methods of Kogler et al, and us.[38,39,41] Briefly, USSCs were transduced with a lentivirus carrying GFP-luciferase gene to track USSC movement in vivo, pSico PolII-eGFP-Luc2 (generously provided by Dr. Glenn Merlino at the National Cancer Institute), cell functionality was evaluated by our group for cell-specific expression and fidelity with the parent USSC phenotype.[42] All experiments used one frozen stock of USSC stem cells.

Glycerol-Induced Interventricular Hemorrhage in Premature Rabbit Pups

Timed pregnant New Zealand white rabbits (Oryctolagus cuniculus) were purchased from Charles River Laboratories Inc. (Wilmington, MA, USA). The premature pups were delivered by cesarean section (Supplementary Fig. S1A) at E29 gestational age (term gestation = 32 days). Newborn premature pups were maintained and fed according to methods published in our previous publications.[38,39,43]

We induced hemorrhage and confirmed presence and absence using sonography (Supplementary Fig. S1B-S1F). The grades of IVH were defined based on the ventricular volume of echogenic area measured (length, breadth, and depth in coronal and sagittal views) as described.[38,39] Hemorrhage was

classified as: (1) no gross IVH, (2) moderate (clot 30-100 mm^3), gross hemorrhage into lateral ventricles with some ventricular enlargement (2 separate lateral ventricles discerned); or (3) severe (clot 100-250 mm^3) IVH with considerable ventricular enlargement (fusion of ventricles into a common chamber) and/or intraparenchymal hemorrhage. After head ultrasound grading, the pups are assigned to 3 groups: (1) Control pups with no IVH, (2) Glycerol-IVH saline injected pups, and (3) Glycerol-IVH USSC injected. We use one premature rabbit pup in each experimental group (no IVH healthy control, IVH saline injected control, and IVH each treatment) for each experimental endpoint from the same litter. The New York Medical College Institutional Animal Care and Use Committee (IACUC) approved all experimental interventions, endpoint sample collections, and laboratory assays.

Multiplex DNA-PCR for Sex Determination

The sex determination was performed using multiplex DNA-PCR with specific male SRY gene and GAPDH control gene amplification simultaneously as shown in Supplementary Fig. S2B. Briefly, the method includes genomic DNA isolation (Cat # 51304, Qiagen DNA-mini-Kit, USA) from a small piece of tissue taken from forebrain coronal slice or ear pinch. The extracted DNA was quantified using Nano-Drop Spectrophotometer ND-2000C (Thermo Fisher Scientific, Waltham, MA, USA). Using 100 ng of genomic DNA, PCR amplification was performed with the rabbit specific SRY gene (AY785433) sense primer 5′-AGCGGCCAGGAACGGGTCAAG-3′ and 5′-CCTTCCGGCGAGGTCTGTACTTG-3′ antisense primer with amplicon size 241 bp, along with rabbit GAPDH gene specific (Accession #L23961) sense primer 5′-TGAACGGATTTGGCCGCATTG-3′ and antisense primer 5′-ATGCCGAAGTGGTCGTGGATG-3′ amplicon size 487 bp. The PCR reaction was performed in 20 µL reaction for a total of 25 cycles. The PCR conditions include denaturation at 98°C for 30 seconds; annealing at 56°C for 45 seconds; and extension 72°C at 1 minute. The amplified DNA products were visualized in 2% agarose gel under UV light and photographed (Supplementary Fig. S2B). The results were recorded, and gender was balanced in each experimental endpoint of the study.

Anatomical Localization of Intracerebroventricular Administered USSCs

USSCs were administered into the lateral cerebral ventricle using coordinates from the Bregma: 1 mm posterior, 4 mm lateral, and 3 mm deep (1×10^6 cells in 10 µL normal saline to each ventricle) as we previously described.[38,39] We confirmed the presence and anatomical location of migrated USSCs in rabbit tissues at different postnatal ages as well as USSC survival and migration as previously described.[38,39]

Rabbit Tissue Collection and Processing

Multiple forebrain parenchymal tissues, cerebrospinal fluid, and plasma samples were collected from the 3 experimental groups (no IVH controls, IVH + saline, and IVH + USSC injected) at postnatal days 3, 7, and 14.[38,39,43] Replicate animal experiments were conducted until the sample size for each treatment category was achieved for all assays performed. Each intervention group was targeted to receive 5 to 6 pups for analysis.

We collected CSF from rabbit pups at postnatal day 3, 7, and 14 via the anterior fontanelle, sample were snap-frozen on dry ice and stored at −80°C until used for ELISA analysis. The SVZ including the GM, CC, and CR was manually dissected under a microscope (as shown in Fig. 7F) from 3 mm coronal slices and were directly snap-frozen on dry ice and stored in −80°C until tissues were processed for RNA isolation and tissue lysates for ELISA and realtime PCR analyses. Forebrain samples were directly processed, fixed, and mounted as a coronal block for immunohistochemistry (IHC) studies described.[38,39,44]

Immunohistochemistry

Immunohistochemical staining was performed, as we previously described.[38,39] The primary antibodies used in the study: PDGFRα (catalog # AF307 NA, R&D Systems, Minneapolis), Olig2+ (catalog # AF2418, R&D Systems, Minneapolis), Ki67+ (catalog # M724029, DAKO/Agilent, Germany), and Nkx2.2+ (catalog # 74.5A5, Developmental Studies Hybridoma Bank, Iowa). The sections were counter stained with DAPI nuclear stain.

CNS Cell Density and Quantification Procedures

Total proliferating cells were identified by labeling coronal sections of the SVZ (CC, CR, and GM) in alternate 40× images at the level of midseptal nucleus with Ki67 antibody (data shown in the Fig. 1J and 1K and Fig. 2J). We counted 2-3 alternate sections in each pup and 5 pups from each experimental group. Data are presented as mean cell count 40× image (mean ± SEM). Early proliferating OLPs were identified by double-labeling coronal sections with PDGFRα and Ki67. Late proliferating OLPs were identified by double labeling the coronal sections with Olig2 and Ki67 antibodies, while maturation of OL progenitors was assessed by double labeling the sections with Olig2 and NKx2.2 antibodies. Quantification was performed by a blinded investigator in a random, unbiased fashion using those microscopic images.

Enzyme-Linked Immunosorbent Assay

The CSF and dissected tissue homogenates from postnatal age 3, and 7 were assessed for TGFβ1, FGF, and IGF protein expression by ELISA method following manufacturer's protocol (catalog # ELH-TGFβ1, and catalog # ELH-bFGF, RayBiotech, Norcross, GA) and for mRNA steady-state levels by PCR among the 3 experimental groups. The results were analyzed in duplicate and averaged for each animal before summarizing the data for final outcome metrics at each postnatal age.

TaqMan Assay for Gene Expression

RNA expression was performed by real-time PCR as previously described.[38,39] Briefly, total RNA was isolated from SVZ dissected tissue from a coronal brain slice taken at the level of the midseptal nucleus. Total RNAs was reverse transcribed to cDNA by using the Superscript First strand Synthesis System for RT-PCR kit (catalog #11904-018, Invitrogen, CA, USA). Gene expression quantification was performed using the HT 7900 ABI (USA) machine. The following rabbit specific TaqMan probes were used for gene expression: TGFβ1 (assay ID: Oc04176122_m1), FGF (assay ID: Oc03396228_m1), IGF1 (assay ID: Oc04096599_m1), p21Cip1 (CDKN1A), assay ID: Oc06761970_m1, p27Kip1 (CDKN1B), assay ID: Oc04097058_m1, p57Kip2 (CDKN2C), assay ID: Oc04707317_g1), KLF4, assay ID: Oc06754906_g1, and CKS2, assay ID: Oc06784843_g1. The realtime PCR analysis

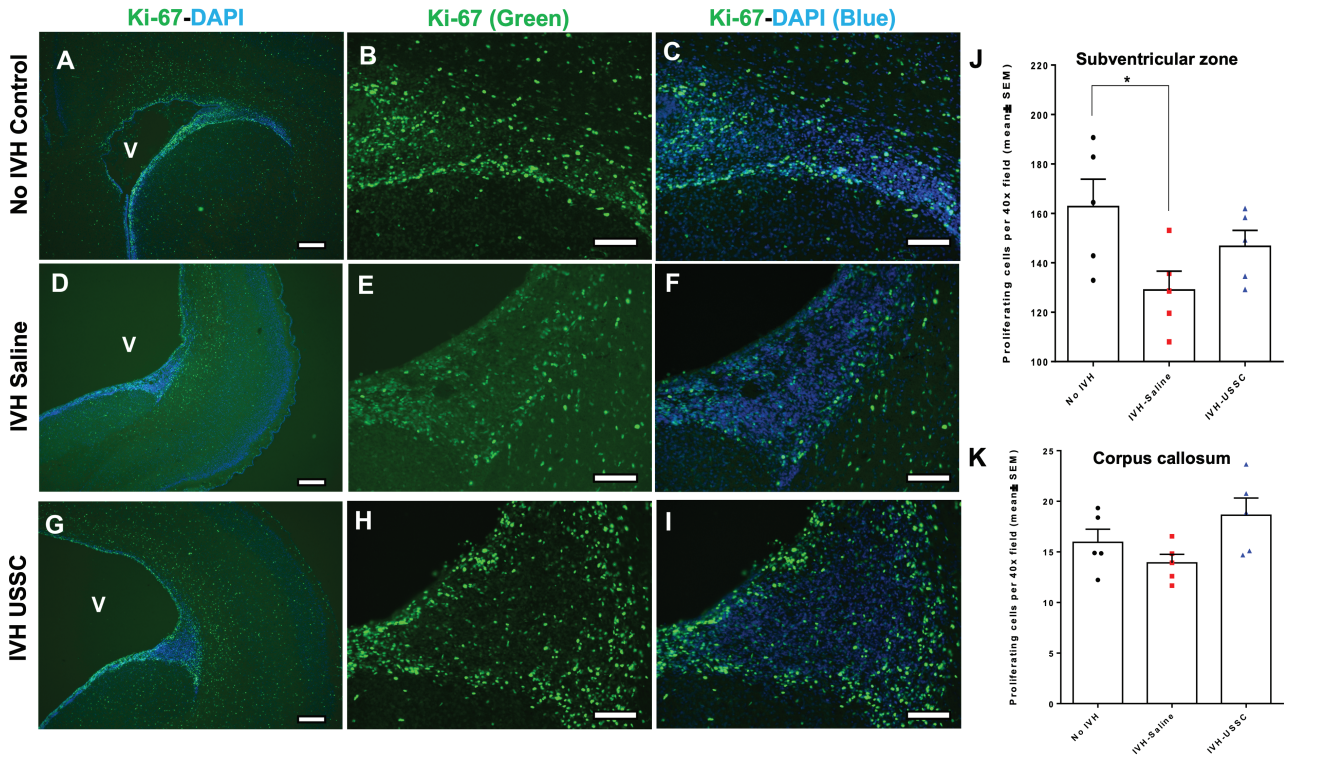

Figure 1. Impaired cell proliferation in the germinal matrix/corona radiata region of the subventricular zone (SVZ) after intraventricular hemorrhage at postnatal day 3. (**A**-**I**) Representative immunofluorescence images labeled with Ki-67 (proliferation marker, green) and counter stained with DAPI (nucleus marker, blue). Low magnification (4×) images from GM/CR (A, D, and G) and high magnification (20×) images with Ki-67 single stain (B, E, and H) and combined Ki-67 with DAPI (C, F, and I) in the 3 experimental groups indicated. Total proliferation immunofluorescence signal was lower in IVH + saline injected pups (middle panel, D-F) compared with no IVH healthy controls (upper panel, A-C) and a recovery in the USSC injected IVH premature pups (bottom panel, G-I). Sample size was 5 in each group, and 2-3 alternate coronal sections were taken at the level of mid-septal nucleus 20 µm sections. Scale bar = 100 µm. Ventricle (V) (**J**-**K**) Quantitative distribution of total proliferating cells in the subventricular zone (SVZ) and corpus callosum (CC). The scatter plot with bar graph showing mean cell density ± SEM among 3 experimental groups. Note: Significantly reduced proliferating cell density after IVH in SVZ but not in CC at day 3 (Control vs. IVH, $P < .05$). USSC treatment shows a trend to increase but not significant in both SVZ and CC; $N = 5$ in each group and cells were counted on 2-3 alternate coronal sections taken at the level of mid-septal nucleus. 20 µm sections.

was performed in duplicate for all postnatal age groups simultaneously.

Statistics and Analysis

To determine differences between the groups in each postnatal age, we used one-way ANOVA to compare treatments. To compare simultaneously, all groups and postnatal ages, we applied 2 way ANOVA with multiple comparisons using GraphPad Prism-6 (GraphPad Software, CA, USA). All post hoc comparisons were done using Tukey multiple comparison testing; values <.05 were considered significant. While gender differences are an important component of biological variation, as there is no published evidence of gender difference causing IVH and in an effort to minimize animal exploitation we did not perform a gender-specific analysis separately. Instead, we balanced the groups with equal representation of both male and females for our datasets.

Results

Intraventricular Hemorrhage Reduced Central Nervous System Progenitor Cell Proliferation in the SVZ but Not in the Corpus Callosum and Corona Radiata During Early Postnatal Development

In this rabbit model of IVH, we showed that IVH occurred in the germinal matrix with attendant injury to the neighboring white matter along with reduced neurogenesis (Supplementary Fig. 1D-1F). As progenitors cells in the GM and ventricualr-SVZ (V-SVZ) are born, migrate, and mature to form the white matter, we focused on this structure to define effects of USSCs after IVH. Overall progenitor cell proliferation at day 3 postnatal age, immunoreactivity of proliferating cells (Ki-67; green) was significantly reduced in IVH pups in the germinal matrix (GM/V-SVZ) compared with no IVH control or IVH pups injected with USSCs (Fig. 1A-1I). Quantitation of overall CNS progenitor cell proliferation in the SVZ showed significantly reduced cell proliferation in IVH pups compared with no IVH healthy controls (Fig. 1J), whereas in the CC and CR, there was a trend to decrease but not significantly (Figs. 1K and 2J). In contrast, USSC-injected IVH pups showed a trend to recovery in all 3 regions, but this did not achieve statistical significance (Fig. 1J and 1K and Fig. 2J). A similar trend was observed at postnatal day 7 in the GM/CR region (Fig. 2A-2I). We further extended our observation to the ventricular zone (VZ) of the lateral ventricular ependymal wall (Fig. 3A-3I), where proliferating (Ki-67 positive) cells were abundent and showed multilayer immunoreactivity in the no IVH (healthy control) group (Fig. 3A-3C top panel) and the USSC-treated IVH pups (Fig. 3G-3I lower panel) compared with reduced proliferating (Ki-67$^+$) cells in the IVH+ saline injected pups (Fig. 3D-3F middle panel) at day

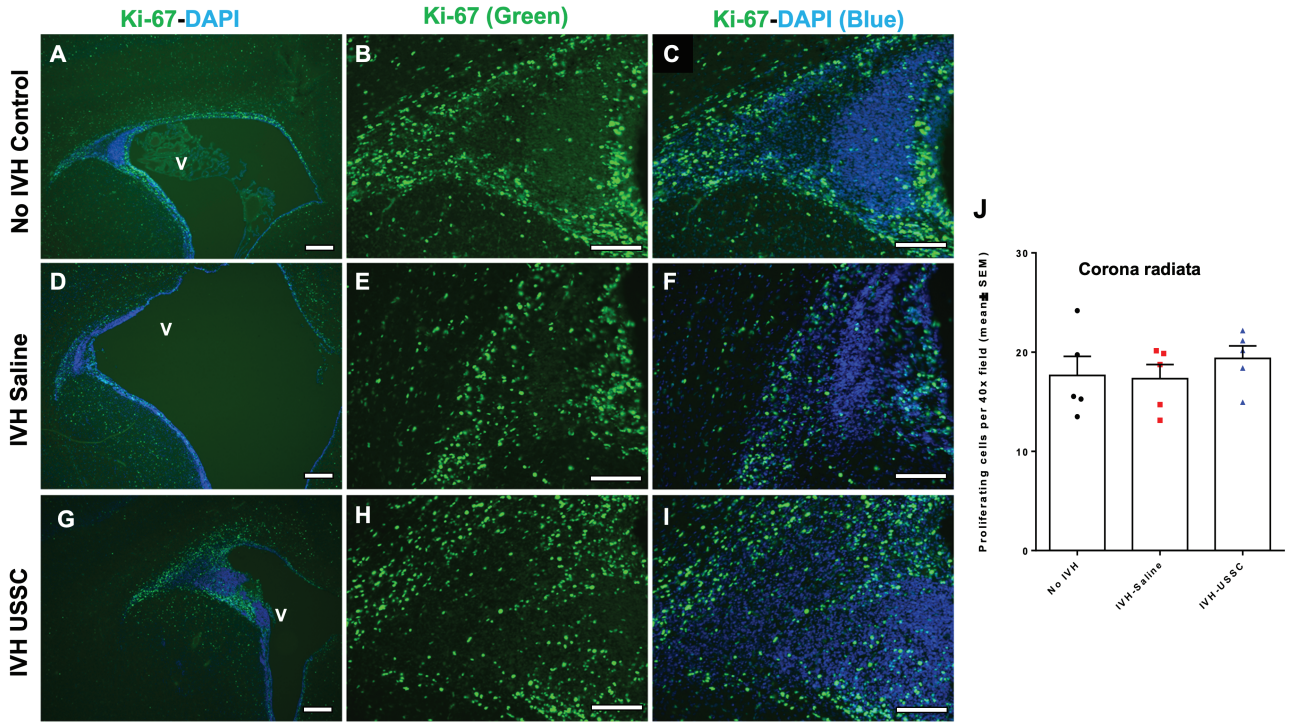

Figure 2. Comparable cell proliferation in germinal matrix/corona radiata region of the subventricular zone after Intraventricular hemorrhage at postnatal day 7. (**A-I**) Representative immunofluorescence images labeled with Ki-67 (proliferation marker, green) and with DAPI (nucleus marker, blue). Low magnification (4×) images from GM/CR (A, D, and G) and high magnification (20×) images with Ki-67 single stain (B, E, and H) and combined Ki-67 with DAPI (C, F, and I) in the 3 experimental groups indicated at postnatal day 7. The proliferation immunofluorescence signal remained slightly reduced at day 7 in IVH + saline injected pups (middle panel: D-F) compared with no IVH healthy controls (upper panel: A-C) and a near recovery to controls in the USSC injected IVH premature pups (bottom panel: G-I). Sample size was 5 in each group, and 2-3 alternate coronal sections were taken at the level of mid-septal nucleus, 20 µm sections. Scale bar = 100 µm. Ventricle (V). (**J**) Quantitative distribution of total proliferating cells in the corona radiata (CR). The scatter plot with bar graph showing mean cell density ± SEM, among 3 experimental groups. Note: The total proliferating cell density in CR was comparable among 3 groups; $N = 5$ in each group and cells were counted on 2-3 alternate coronal sections taken at the level of mid-septal nucleus.

3. This indicated that USSCs conferred recovery of cell proliferation in the VZ.

USSC Administration Increased *Early* and *Late* Oligodendrocyte Progenitor Cell Proliferation After IVH

We previously reported that USSC administration improved myelination and neurobehavioral performance in premature rabbit pups after IVH.[38] Therefore, we sought to test whether IVH mediated pathological mediators would contribute to changes in OPC proliferation and maturation by assessing changes in proliferating early and late OL density in 3 experimental groups. During normal development, progenitor cells typically divide in 3 primary locations: (1) ventricular zone (VZ), (2) inner SVZ, and (3) OSVZ. In order for myelination to occur, the following proliferation and maturation sequence must occur: (1) proliferation of early oligodendrocyte precursor cells (PDGFRα$^+$), (2) differentiaton into late oligodendrocyte precursor cells (Olig2$^+$, Nkx2.2$^-$), then (3) differentiation into immature myelinating oligodendrocyte (Oligo2$^+$-Nkx2.2$^+$-MBP$^-$) and finally, progression to myelinating oligodendrocytes Olig2$^+$-NKx2.2$^+$-MBP$^+$.[1,2] We quantified early oligodendrocyte proliferation as double-positive Ki-67$^+$ and PDGFRα+ cells and caliculated cell densities of these subtype cells in forebrain coronal sections ($n = 5$-8 ea) at day 3.

We found significantly reduced *early* OLP (Ki-67+ PDGFRα$^+$) SVZ cell density in IVH+ saline injected pups compared to no IVH controls. In contrast, there was a significant increase in proliferating cell density in the IVH + USSC-treated pups compared with the IVH + saline pups on postnatal day 3 ($P < .05$ for both comparisons, $n = 5$ pups in each group; Fig. 3J).

Early oligodendrocyte PDGFRα$^+$ precursor cells proliferate in the SVZ and migrate to the CC and CR to continue to mature into *late* oligodendrocyte precursor cells. To determine if this progression occurred, we assessed *late* oligodendrocyte precursor (Olig2$^+$-Ki67$^+$ double positive) specific cell proliferation in the corpus callosum (CC) and corona radiata (GM/CR). In Fig. 4A-4F, on postnatal day 7, *late* oligo proliferation was reduced in the corona radiata (GM/CR) after IVH (Fig. 4C (10×) and D (40×) vs. A-B: Olig2-positive cells [red]; Ki-67 [green]; dual stained [yellow]) but returned to levels seen in healthy controls after USSC treatment (Fig. 4A and 4B vs. Fig. 4E and 4F).

In the corpus callosum, *late* proliferating OLs were reduced (yellow cells) after IVH compared with healthy controls (Fig. 4G-4H vs. Fig. 4I-4J), while USSC-treated IVH pups (Fig. 4G-4H vs. Fig. 4K-4L) recovered by day 7. This trend was observed in both lateral (Fig. 4A-4F) and medial sides of the CR ventricles (Supplementary Fig. 1G-1L). Cell density quantitation of double-labeled Olig2$^+$-Ki67$^+$ cells in the CC and CR regions at day 3 is shown in Fig. 3K ($P < .05$ for both comparisons, $n = 5$ pups each group). In summary, we observed recovery of the IVH-induced reduction of both *early*

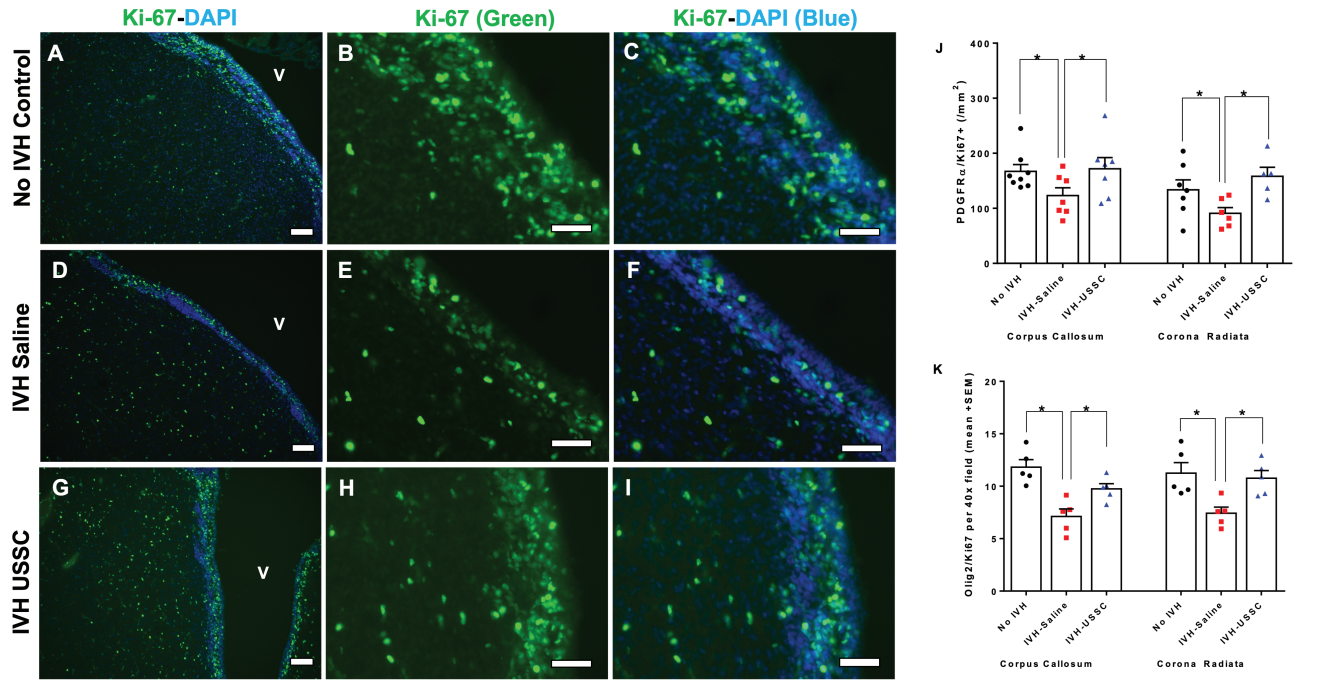

Figure 3. Impaired proliferation of central nervous system progenitor cells in the ventricular zone (VZ) after IVH at early postnatal age day 3. (**A-I**) Representative immunofluorescence images labeled with Ki-67 (proliferation marker, green) and counter stained with DAPI (nucleus marker, blue). Low magnification (10×) images from the ventricular zone (A, D, and G) and high magnification (40×) images with Ki-67 (green) single stain (B, E, and H) and combined Ki-67 with DAPI (C, F, and I) in the 3 experimental groups indicated at postnatal day 3. Total proliferation immunofluorescence signal in the ventricular zone was lower in IVH + saline injected pups (middle panel, D-F) compared with no IVH healthy controls (upper panel, A-C) and a recovery in the USSC injected IVH premature pups (bottom panel, G-I). Sample size was 5 in each group, and 2-3 alternate coronal sections were taken at the level of mid-septal nucleus 20 μm sections. Scale bar = 100 μm. Ventricle (V). (**J-K**) Increased density of proliferative early OL (PDGFRα+) and late OL (OLIG-2+) progenitor cells after USSC stem cells administration in IVH. (**J**) The scatter plot with bar graph showing quantitative distribution of PDGFRα positive early oligodendrocyte lineage progenitor cell proliferation in the corpus callosum (CC) and corona radiata (GM/CR). Significantly reduced early OL proliferation observed after IVH (Control vs. IVH, $P < .05$ in both CC and GM/CR). USSC treatment significantly enhanced proliferation (IVH + saline vs IVH + USSC, $P < .05$ in both CC and GM/CR). Sample size of 5-8 in each group and cells were counted on 2-3 alternate coronal sections taken at the level of mid-septal nucleus and stained with PDGFRα combined with Ki-67 antibody; counter stained with DAPI nuclear stain at postnatal day 3. (K) The scatter plot with bar graph showing quantitative distribution of OLIG2 positive late oligodendrocyte lineage progenitor cell proliferation in the corpus callosum (CC) and corona radiata (GM/CR).

and *late* OLPs after USSC treatment in the CR and CC on postnatal days 3 and 7, respectively.

USSC Administration Increased *Myelinating* OPC Proliferation After Intraventricular Hemorrhage

Previous studies reported a maturational arrest in the oligodendrocyte lineage from precursor to myelinating OLs after IVH.[1,2,4,45] Therefore, we sought to determine whether the altered *early* and *late* oligodendrocyte proliferation seen in USSC-treated IVH pups would also affect the maturation and myelination process. To asses this we performed immunohistochemical analysis of Olig2+ and Nkx2.2^{+} double positive (immature myelinating oligodendrocyte) cells for mature myelinating oligodendrocyte on coronal sections from day 7.

We found reduced immature myelinating oligodendrocyte (Oligo2+ [green]-Nkx2.2+ [red], double positive [yellow]) after IVH in both CR and CC regions compared to the no IVH healthy controls (Fig. 5A and 5B vs. C-D for CR and G-H vs. I-J for CC). This reduction recovered in USSC-treated IVH pups (Fig. 5C-5D vs. E-F for CR and I-J vs. K-L for CC). This data further supports the argument that after USSC treatment of IVH, increased *late* Olig2 proliferation and maturation into immature OLs contributes to the improved myelination seen in our previous reports.

USSC Administration Increased Early Postnatal Expression of TGFβ1 and FGF2 After IVH

Multiple growth factors normally secreted into the CSF, brain parenchyma, and meninges interact with CNS progenitor cells in the VZ through the brain-CSF interface and contribute cell fate by generating molecular signals that stimulate proliferation, migration, and maturation during postnatal development.[11] USSCs produce 1156 known proteins, 31 of which are established growth factors. In addition to this robust paracrine function, USSC also showed more regenerative functions than mesenchymal cells.[35,36,41,42]

To determine whether there was a correlation between expression of growth factors known to be involved in OL progenitor cell population survival, proliferation, and differentiation, we administered USSC and quantified expression of relevant growth factors: TGFβ1, FGF2, and IGF in the brain parenchyma. We measured TGFβ1 protein levels in CSF at postnatal days 3, 7, and 14 and identified a trend toward higher levels of TGFβ1 in healthy controls compared to IVH pups on all postnatal points (days 3, 7, and 14) ($n = 6$, $P < .05$ only for day 7 pups; Fig. 6A and 6C). Moreover, in all groups, there was a gradual decrease in TGFβ1 protein levels from days 3 to 14. In USSC-treated IVH pups, CSF TGFβ1 protein levels were significantly recovered toward normal control expression levels on postnatal days 3, 7, and 14 ($n = 6$, $P < .05$

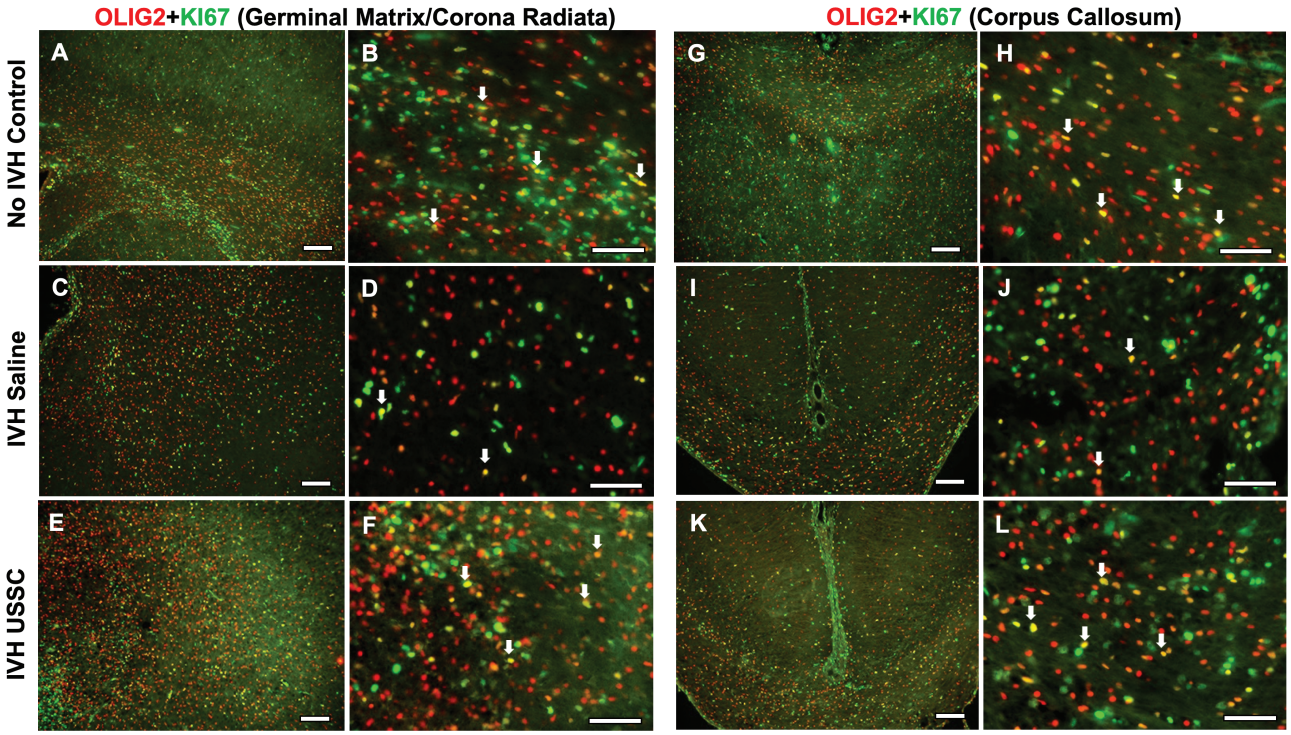

Figure 4. USSC administration increased OLIG2 positive late progenitor cell proliferation in the GM/CR and CC after IVH on day 7. (**A**-**F**) Representative immunofluorescence images shown double-labeled coronal sections with Olig2 (red) and Ki-67 (green) in GM/CR. Low magnification images (10×) from healthy controls (A), IVH + saline (C) and USSC treated IVH pups (E). High magnification (40×) images double-labeled Ki67, Olig2 from controls (B), IVH + saline (D) and USSC treated IVH pups (F). Reduced double-positive immunosignals of OLIG2 with Ki-67 (yellow) in IVH (C, D) compared with both no IVH control (A, B) and IVH + USSC treated pups (E, F) in GM/CR of the SVZ. Double-positive cells shown with an arrow. Sample size of 5 in each group with 2-3 alternate coronal sections taken at the level of mid-septal nucleus of the forebrain for each pup; 20 µm sections. Scale bar = 100 µm. (**G**-**L**) Representative immunofluorescence images shown double labeled with Ki67-Olig2 in the corpus callosum. Low-magnification images (10×) from healthy controls (G), IVH saline (I), and USSC-treated IVH pups (K). High magnification (40×) images double-labeled Ki67-Olig2 from healthy controls (H), IVH + saline (J), and USSC-treated IVH pups (L). Reduced double-positive immunosignals of OLIG2 with Ki-67 (yellow) in IVH (I, J) compared with either no IVH control (G, H) or in IVH + USSC-treated pups (K, L) in CC region. Double-positive cells shown with an arrow. Sample size of 5 in each group with 2-3 alternate coronal sections taken at the level of mid-septal nucleus of the forebrain for each pup; 20µm sections. Scale bar = 100 µm.

across all comparisons; Fig. 6A). We next applied a 2-way ANOVA for CSF protein analysis, because there is a higher likelihood that sequential sampling of CSF would prove useful in a clinical setting based on future studies in animals without needing to sacrifice them. The data for simultaneous comparison of groups and postnatal ages, indicated significant differences in TGFβ1 protein expression for IVH versus USSC treatment for days 3 and 14 ($P < 0.05$) but not for day 7 (IVH vs. USSC for days 3 and 14, $P < .05$) At day 7, the TGF protein levels were was significantly different in Control versus IVH ($P < .05$; Fig. 6C).

To further corroborate the protein data, we investigated steady-state levels of TGFβ1 isoform-specific mRNA expression in dissected tissue samples on postnatal days 3, 7, and 14. The real-time Taqman mRNA gene expression analysis confirmed the protein pattern in the 3 experimental groups on postnatal day 3 ($n = 5$, $P < .05$) but not on days 7 and 14 (Fig. 6B). Falling levels of TGFβ1 occur concurrently with the reduced number of early proliferating OLPs in the SVZ.

We next investigated CSF FGF2 protein and SVZ mRNA expression and found a trend toward reduced CSF protein levels of FGF2 with postnatal age but no effect of IVH or USSC treatment compared with healthy controls ($n = 4$; P-ns; Fig. 6D). In the SVZ, FGF2 mRNA expression was higher than in the IVH + Saline group after USSC treatment only at day 3 ($n = 5$, $P < .05$, IVH vs. USSC; Fig. 6E).

We assessed IGF mRNA expression and found no changes in expression either across postnatal ages or between 3 experimental groups (Fig. 6F). Taken together, the data are consistent with reports identifying an early role of growth factors (TGFβ1 and FGF2) in the regulation of oligodendrocyte cell lineage, proliferation and improved myelination in this rabbit model of IVH.

Cell Cycle Regulating Genes and Oligodendrocyte Lineage Fate Through Regulation of TGFβ1 and FGF2 Expression

To determine whether cellular mechanisms through which growth factors mediate cell cycle regulation after injury may control the fate of progenitor cell proliferation and maturation, we evaluated mRNA levels of mitotic cell cycle regulator genes (G1/S transition) associated with oligodendrocyte lineage in the germinal zone. Early G1 mitogens that regulate entry into S-phase cell cycle include: (1) CDKN1A (p21Cip1), (2) CDKN1B (p27kip1), (3) CDKN2C, (4) KLF4, and (5) CKS2.

Steady-state levels of CDKN1A (p21Cip1) and CDKN2C mRNA were not significantly different at any time point or condition (Fig. 7A and 7C). However, CDKN1B mRNA was significantly higher in IVH pups compared with no IVH controls on postnatal day 3 ($P < .05$; Fig. 7B) while USSC-treated IVH pups had significantly reduced CDKN1B mRNA

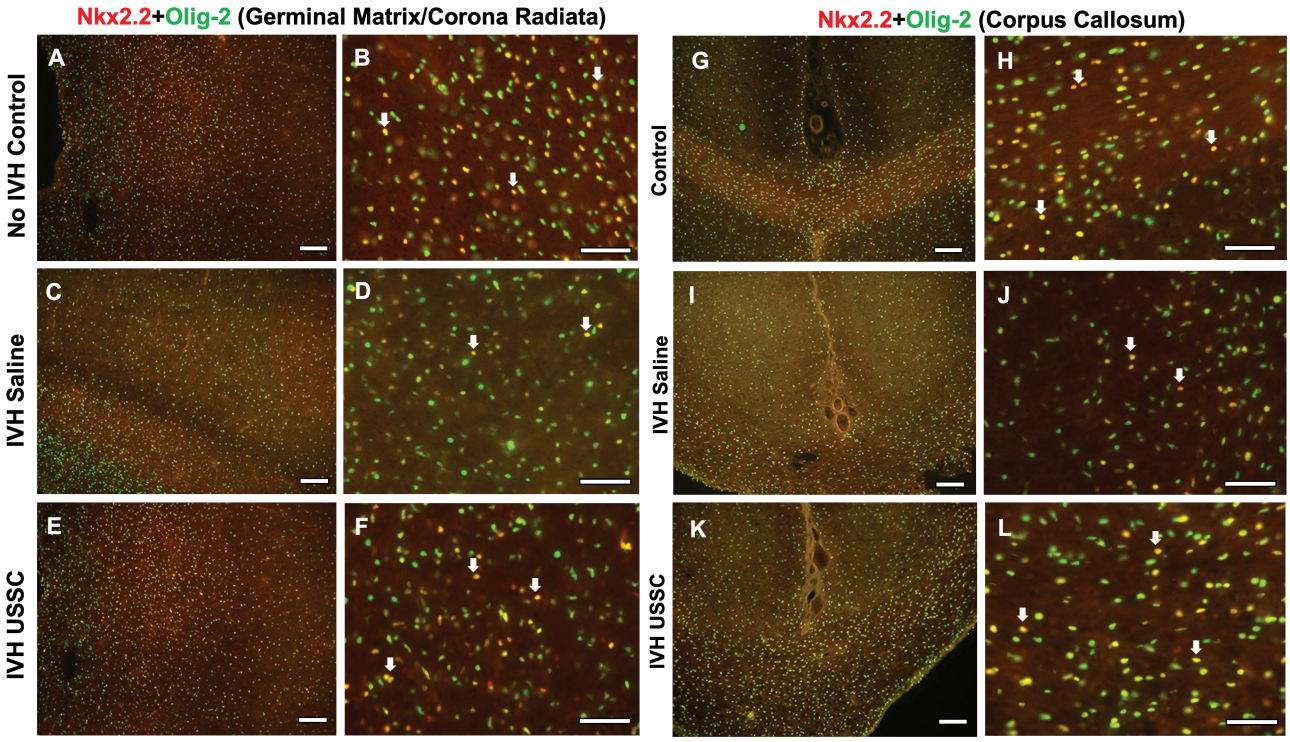

Figure 5. USSC administration increased NKX2.2 + Olig-2 positive immature myelinating oligodendrocyte progenitor cells after IVH in the GM/CR and CC after IVH. (**A**-**F**) Representative immunofluorescence images of immature myelinating OL (double-labeled Olig2-NKx2.2) in the GM/CR. Low-magnification images (10×) and high-power magnification (40×) double-labeled Olig2-NKx2.2 from healthy controls (B), IVH + saline (D), and USSC-treated IVH pups (F). Reduced double-positive immunosignals of OLIG2 + NKx2.2 (yellow) in IVH (C, D) compared with both no IVH control (A, B) and IVH USSC-treated pups (E, F) in the GM/CR region of the forebrain. Double-positive cells shown with an arrow. Sample size of 5 in each group with 2-3 alternate coronal sections taken at the level of mid-septal nucleus of the forebrain for each pup; 20 µm sections. Scale bar = 100 µm. (**G**-**L**) Representative immunofluorescence images of immature myelinating OL (double labeled with Olig2-NKx2.2) in the CC. Low-magnification images (10×) from controls (G), IVH + saline injected (I), and USSC-treated IVH pups (K). High-power magnification (40×) double-labeled Olig2-NKx2.2 from controls (H), IVH + saline (J), and USSC-treated IVH pups (L). Reduced double-positive immunosignals of OLIG2 + NKx2.2 (yellow) in IVH (I, J) compared with either no IVH control (G, H) or IVH + USSC-treated pups (K, L) in CC region of the forebrain coronal sections. Double-positive cells shown with an arrow. Sample size of 5 in each group with 2-3 alternate coronal sections taken at the level of mid-septal nucleus of the forebrain for each pup; 20 µm sections. Scale bar = 100 µm.

expression compared with IVH + saline injected pups ($n = 5$, $P < .05$) (Fig. 7B). This data are consistent with an interpretation that after USSC administration for IVH, the increased expression of TGF-β1 and FGF2 are associated with reversal of CDKN1B mediated G1 arrest of progression to S-phase mitosis at day 3.

During development, the protein KLF4 is essential for self-renewal and maintenance of stem cell populations such as in mesenchymal stem cells (MSCs).[46] KLF4 induces Myc expression, which is a positive stimulator of cell division in the presence of mitogens like NT3, PDGF and FGF. Therefore, it is possible that an increase of KLF4 would be associated with OL proliferation through Myc after USSC administration. We examined KFL4 mRNA expression levels and found a trend to reduced KFL4 mRNA levels in IVH pups compared with no IVH healthy controls at day 3 and a trend toward recovery of levels in pups treated with USSCs (Fig. 7D; P - ns).

Further, it is known that the KLF4 induce Myc expression, is a positive stimulator of cells to divide in the presence of mitogens like NT3, PDGF, and FGF Therefore, it suggests that the increase of KLF4 might be associated with OL proliferation through Myc after USSC administration. Another cell cycle regulator, CKS2 subunit, promotes proliferation, and suppresses apoptosis. We found no difference after IVH + saline versus IVH controls while USSC treatment after IVH showed a trend toward increased expression at postnatal age day 3 but not 7 (Fig. 7E). In summary, while trends in cyclin gene levels were of interest, the data were inconclusive with regard to their role after single dose of USSCs at reversing the reduced cell proliferation observed in IVH pups as assessed by Ki-67 staining in different regions of SVZ.

Discussion

Intraventricular hemorrhage is a life-altering complication of prematurity, and its pathogenesis is complex and multifactorial in nature. Despite major efforts made for its prevention, no successful treatment is available. Previously, we demonstrated that exogenous USSC infusion, enabled recovery of WMI after IVH by enhanced myelination, reduced gliosis, decreased hydrocephalus, and improved locomotor function.[38,39] In the current study, we extend those observations and show that in rabbit pups after IVH, ICV infusion of USSCs elicit growth factor release into the CSF and brain parenchyma and facilitated apparent recovery of oligodendrocyte progenitor cell proliferation and maturation coincident with improved myelination.[38,39] Curiously, we did not detect changes in common cyclin-related genes after IVH + USSC treatment compared to controls.

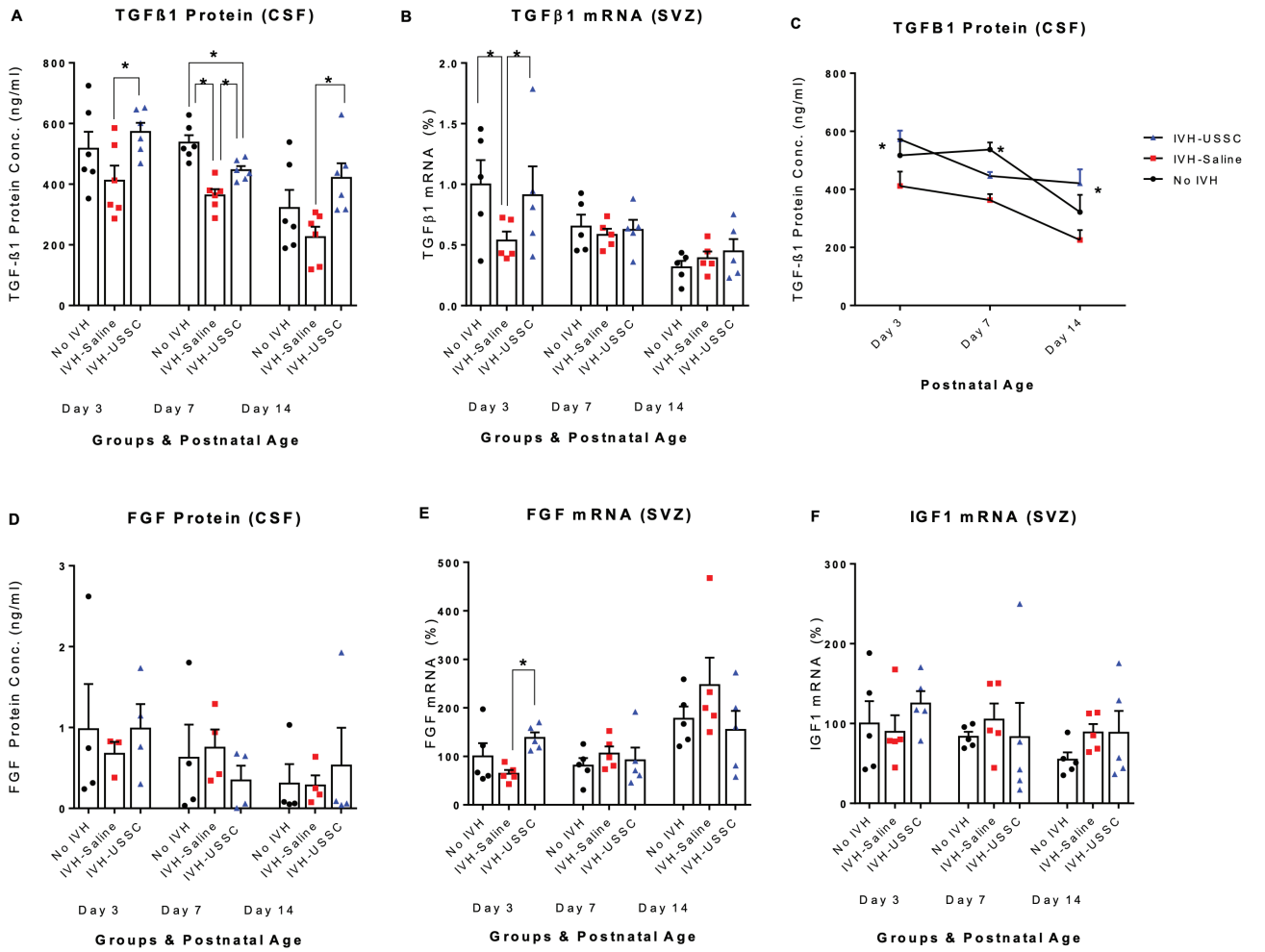

Figure 6. USSC administration altered the early postnatal expression of growth factors TGF-β1 and FGF after IVH. (**A**-**C**) Scatter plot with bar graph and Lane chart showing the expression of TGF-β1 protein and gene expression in CSF and SVZ dissected tissue mRNA. (A) Scatter plot with bar graph showing decreased TGF-β1 protein levels in the CSF of IVH pups compared to control pups, whereas USSC-treated pups showed significantly increased expression at postnatal days 3, 7, and 14. (*P < .05, Ctrl vs. IVH at day 7, and IVH vs. USSC pups at day 3, 7, and 14, n = 5-6 pups in each group). The data represents mean ± SEM (ng/mL). Assay using ELISA kit (Ray Biotech., catalog # ELH-TGFβ1). (B) Scatter plot with bar graph showing decreased TGF-β1 mRNA expression in IVH pups compared to control pups, whereas USSC-treated pups showed significantly increased expression at postnatal day 3. (*P < .05, Ctrl vs. IVH as well as IVH vs USSC pups at day 3, whereas other postnatal ages were comparable in mRNA expression, n = 5 pups in each group). (C) Line graph showing falling TGF-β1 protein levels in the CSF over the first 2 postnatal weeks independently of treatment assignments. Two-way ANOVA showed significant differences for IVH vs. USSC treatment for day 3 and day 14 (P < .05 for both) and also for control vs IVH group at day 7 (P < .05). (**D**-**E**) Scatter plot with bar graph showing the expression of FGF protein and gene expression in CSF and dissected tissue RNA. (D) Scatter plot with bar graph showing decreased FGF protein levels in the CSF in IVH pups compared to control pups, whereas USSC-treated pups showed a trend to increase values at postnatal day 3. All comparisons were not significant, n = 4 pups in each group). The data represents mean ± SEM (ng/mL). (E) Scatter plot with bar graph shows decreased FGF mRNA levels in IVH pups compared to control pups, whereas USSC-treated pups showed significantly increased values at postnatal day 3. (*P < .05, IVH vs USSC pups at day3, whereas other postnatal ages were comparable in mRNA expression, n = 5 pups in each group). (**F**) Scatter plot with bar graph showing the expression of IGF1 mRNA levels in dissected tissue that is comparable at all postnatal ages. The data represents mean ± SEM; for each group for 3 postnatal days 3, 7, and 14, n = 5 pups in each group.

The VZ and SVZ contains neuroglial progenitor cells which have the capacity for proliferation and regeneration of new cells after various types of brain injuries. As shown in Figs. 1-3, after IVH and at postnatal day 3, overall OL progenitor cell proliferation was significantly reduced in the germinal matrix (GM) and the ventricular region of the lateral ventricular zone. This reduction was partially recovered in IVH pups who received USSC infusion. Importantly, in the CC and CR, the total proliferation trended toward reduction, but it was not statically significant compared to either controls or USSC-treated pups (Figs. 1K and 2J). These data indicate that IVH reduced overall progenitor cell proliferation primarily in the germinal zone (GM and V-SVZ) where USSCs provided a salutary effects.

Stem cells hold therapeutic promise serving an apparent paracrine effect that modulates proliferation and differentiation of endogenous cell tissue.[47,48] This observation is consistent with previous models of stem cell therapy where stem cell secretomes affect recovery from various injuries.[49] The observation that IVH reduces overall cell proliferation in the VZ and SVZ raises the possibility that reduced total progenitor cell proliferation after IVH is due to a reduction in a specific lineage of glial or neuronal cells. Oligodendrocyte lineage is the most studied progenitor cell in the IVH-injured developing brain where the magnitude of deficit in OL lineage is proportional to the deficits in CNS myelination. Therefore, our current focus was on the fate of oligodendrocyte lineage.

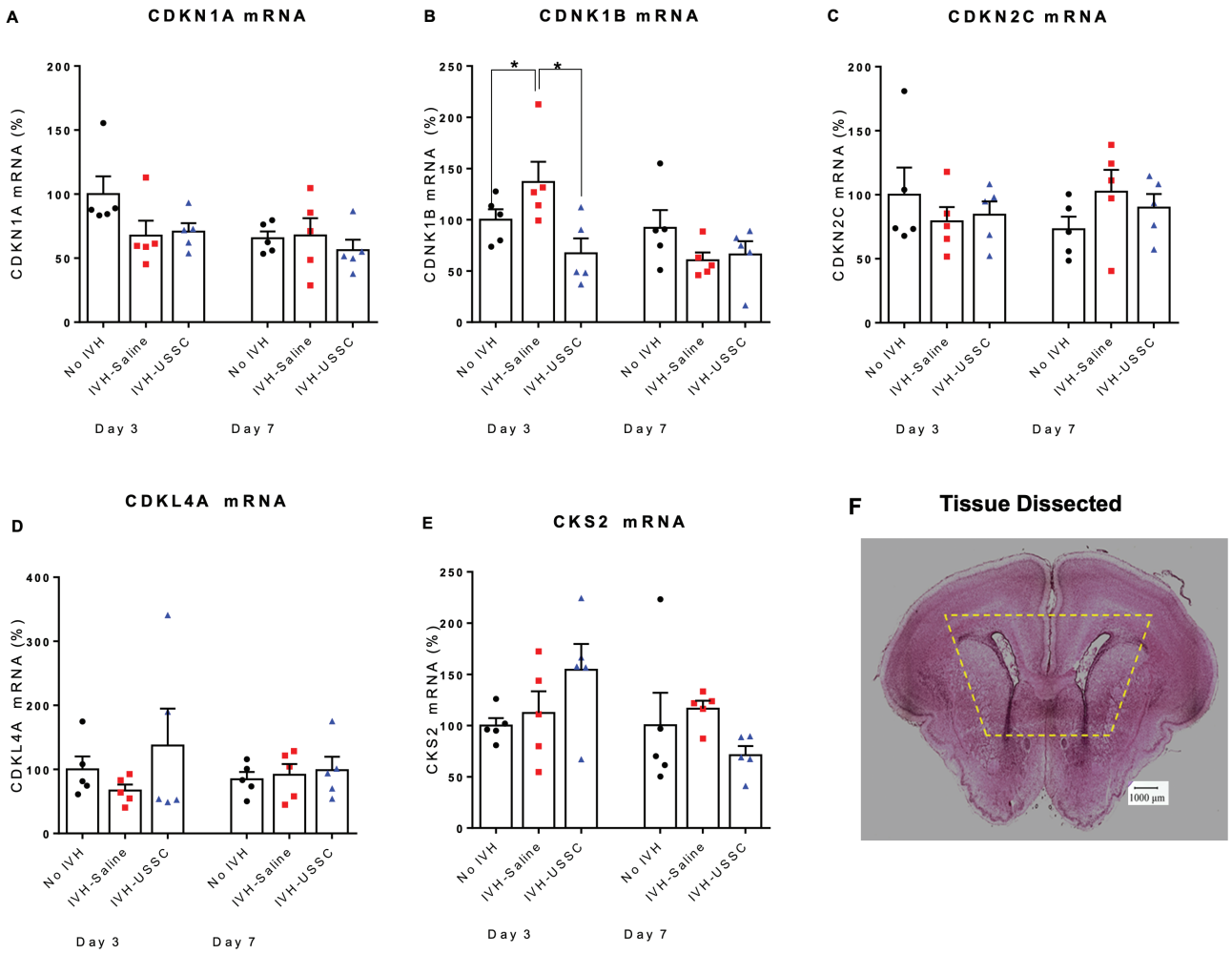

Figure 7. Scatter plot with bar graph showing the cell cycle regulated gene mRNA levels after USSC administration in IVH. (**A**) Scatter plot with bar graph shows comparable CDKN1A (p21) mRNA levels in healthy controls, IVH saline and USSC-treated IVH pups at postnatal days 3 and 7. All groups were comparable in mRNA values, $n = 5$ pups in each group. (**B**) Scatter plot with bar graph shows increased CDKN1B (p27) mRNA expression in IVH pups compared to control pups, whereas USSC-treated pups showed significantly decreased expression at postnatal day 3. (*$P < .05$, Ctrl vs. IVH as well as IVH vs. USSC pups at day 3; other postnatal ages days 3 and 7 were comparable in mRNA values, $n = 5$ pups in each group). (**C**) Scatter plot with bar graph shows comparable CDKN2C mRNA levels in healthy controls, IVH and USSC-treated pups at postnatal days 3 and 7. All groups were comparable in mRNA values, $n = 5$ pups in each group. (**D**) Scatter plot with bar graph shows comparable KLF4 mRNA levels in healthy controls, IVH, and USSC-treated pups at postnatal days 3 and 7. All groups were comparable in mRNA values, $n = 5$ pups in each group. The USSC administration in IVH pups showed a trend to increase compared with IVH saline group. (**E**) Scatter plot with bar graph shows comparable CKS4 mRNA levels in healthy controls, IVH, and USSC-treated pups at postnatal days 3 and 7. All groups were comparable in mRNA values, $n = 5$ pups in each group. (**F**) Representative hematoxylin and eosin (H&E) stained coronal section taken at the level of mid-septal nucleus showing landmarks of dissected areas of coronal tissue used for RNA isolation and TaqMan gene expression assay; 20 µm sections.

We found that *early* and *late* oligodendrocytes (PDGFRα+ and Olig2+) cell lineage showed significant recovery of impaired proliferation seen in IVH pups after treatment with USSC (Figs. 3J and 3K, 4, and 5). This suggests that the control of proliferation, survival, and differentiation of progenitor cells in developing tissues can be altered by USSCs via the integration of multiple extrinsic/intrinsic signals (growth factors, cytokines, less inflammation, etc.) identified in other in vitro and in vivo studies.[20,22,24,50]

To identify whether USSC secreted or induced representative neurotrophic growth factors, we characterized the levels of TGFβ1, FGF2, and IGF. These bioactive signal molecules peak at different postnatal stages of oligodendrocyte cell lineage, proliferation, and differentiation. For example, the TGFβ family of proteins are multifunctional growth factors. Where TGFβ1 is involved in: (1) cell proliferation and maturation,[15,51] (2) limiting proliferation of oligodendrocyte progenitor cells thus promoting oligodendrocyte differentiation and maturation,[15] and (3) can serve as a neuroprotective growth factor improving axonal recovery from chronic nerve injury.[23] Insulin growth factors (IGF1 IGF2) promote receptor-mediated proliferation of progenitor cells and maturation in both in vitro and in vivo experiments.[11,21,22,52-54] Fibroblast growth factor-2 (FGF2) also promotes proliferation of oligodendrocyte precursor cells and, depending on the receptor through which it is mediated, augments in vitro oligodendrocyte progenitor differentiation and maturation.[21,52]

We observed higher TGFβ1 expression at the early postnatal age (3 days) and a subsequent decline at the time of peak myelination at days 7 to 14 in healthy control pups (Fig. 6A-6C), but no significant changes in either IGFs. In contrast, TGFβ1 levels were lower in IVH+ saline pups but

recoverd in IVH+ USSC-treated pups indicating that USSCs can alter TGFβ1 expression which in turn may contribute to the recovery of oligodendrocyte cell function during forebrain development (Fig. 6A-6C) along with other mechanisms of recovery. Our data on FGF2 expression showed attenuation of decreased levels at early postnatal day 3 in USSC-treated IVH pups compared to IVH+ saline pups, suggesting a role for FGF2 involvement in the same oligodendrocyte differentiation processes as TGFβ1 (Fig. 6D-6E). Taken together the changes of TGFβ1 and FGF2 expression in the CSF and brain parenchyma after IVH+ USSCs are consistent with mechanistic beneficial effects of USSCs on various stages of oligodendrocyte cell lineage and the subsequently improved myelination.[38,39]

During development, various growth factors are involved in oligodendrocyte progenitor cell proliferation in a time-critical manner where controlled expression of cell cycle genes govern entry and exit of proliferation. To gain insight into putative mechanism patterns, we examined the simultaneous correlation between oligodendrocyte proliferation, changes in relevant growth factors (TGFβ1 and FGF2 expression) and S-phase cell cycle regulated molecules p21(CDKN1A), p27(CDKN1B), p57(CDKN1C), as well as the stem cell self-renewal necessary molecule KLF4.

Our cell cycle analysis data showed a statistically significant increase in p27Kip1 (a cell cycle inhibitor) in IVH pups compared to healthy controls (Fig. 7B). Although whole tissue was examined, this change is consistent at least in part, with the observed reduction in TGFβ1 and FGF levels causing a G1 arrest of proliferation of maturing oligodendrocytes. This interpretation is further corroborated by observations of recovery of TGFβ1 and FGF expression (both protein and mRNA levels) after USSC administration including a parallel recovery of *early* and *late* OLP proliferation (Figs. 4, 5, and 6 data). Moreover, additional data indicating that a major regulator of cell cycle inhibition P27Kip1[26-28] was increased after IVH and remained at control levels after USSC treatment on day 3 (Fig. 7B) adds to this thesis. KLF4 mRNA (a self-renewal and maintenance of stem cell population factor) was unaffected by IVH or after USSC treatment (Fig. 7D). While only P27Kip1 changed significantly in this limited experiment, these data inform further exploration of multiple other related transcriptional factors like Oct4, Sox2, and cMyc all of which are known regulators of cell cycling and stem cell self-renewal and maintenance during development.

Migration of USSCs to areas of IVH-induced injury is associated with less severe hydrocephalus plus improved motor function.[38] We speculate that hCB USSCs may be a preferred choice compared to MSCs, as they are more primitive and do not cause rejection in xenographic transplantation. Other putative advantages over MSCs are that USSCs possess a higher regenerative and neuroprotective potential as shown in multiple CNS injury models.[30,38,39,41,42] Beyond these findings, we selected USSCs, because they release multiple growth factors and cytokines.[36,55] And, as seen in the current report many of these factors change in tandem with known changes in cell lineage and differentiation of multiple CNS progenitor cells in the SVZ both during development and during CNS repair after injury.[47,48]

The principle limitations of this study reside in the correlative nature of our interpretation of USSC-induced changes in growth factors, cell division, and differentiation as extrapolated from prior reports of normal and IVH-injured brain development. Nevertheless, to validate cell and molecular pathways in vivo will require gene knockout studies, specific factor receptor blocking and/or cell culture experiments. Viewed somewhat differently, to translate the use of USSCs into a relevant clinical therapy, it may not require precise examination of every combinatorial, temporal, or mechanistic possibility that fully characterize how USSCs affect recovery from IVH. Perhaps, the most important conceptual focus of future work should be to establish the long-term safety of these naturally circulating human umbilical cord cells after being grown in culture as a "living therapy" that adapts to the local changes in the tissue microenvironemnt.[49]

In summary, our USSC results indicated that (TGFβ1 and FGF2 but not IGF) growth factor expression correlates with recovery of oligodendrocyte lineage proliferation and maturation after IVH as well as the removal of cell cycle depression through P27Kip1 overexpression (G1 to S-phase inhibition). A P27Kip1 reversal of G1 cell cycle arrest of OL progression to S-phase appears to be a novel contributing feature of reduced myelination after IVH. Since all IVH models show substantial cell death and OL differentiation arrest in early postnatal ages, these "living therapy" observations offer new insights into pathways amenable to interventions using USSCs as adjuvant agents. These effects and other features of the cell line offer the possibility that USSCs have translational potential as therapy in preterm neonates.

Acknowledgements

We thank Rita Daly for proofreading the manuscript and for technical assistance with images. We acknowledge support from the New York Medical College Seed Grant program as well as sustaining funds from the Department of Pediatrics.

Funding

This study was supported by a Boston Children's Health Physicians' Neonatal Division pilot grant for stem cell research (GV and EFL), Seed grant funding, Touro Universities System (GV), and in part by the Pediatric Cancer Research Foundation (MSC).

Conflict of Interest

The authors declare that the research was conducted in the absence of any commercial or financial relationships that could be construed as a potential conflict of interest.

Data Availability

The raw data generated from each experiments that support our research findings presented in this study are available from the senior authors and corresponding author upon acceptable request based on institutional policy.

Author Contributions

G.V, D.A.F: Conception, design, performed experiments, assembly, analysis, interpretation of the data and wrote the manuscript. E.F.L, S.S, M.S.C: Conception, data interpretation,

manuscript writing, financial support, and approval of the manuscript. Y.L, F.H, K.H: USSC isolation, labeling, and BLI imaging and quantification. F.H, A.M, D.P, D.S, S.A.N, K.H: Animal care, sample collection, immunostaining, cell count, neurobehavioral study, and imaging.

Supplementary Material

Supplementary material is available at *Stem Cells Translational Medicine* online.

References

1. Back SA, Luo NL, Borenstein NS, et al. Late oligodendrocyte progenitors coincide with the developmental window of vulnerability for human perinatal white matter injury. *J Neurosci*. 2001;21(4):1302-1312. https://doi.org/10.1523/JNEUROSCI.21-04-01302.2001
2. Dummula K, Vinukonda G, Chu P, et al. Bone morphogenetic protein inhibition promotes neurological recovery after intraventricular hemorrhage. *J Neurosci*. 2011;31(34):12068-12082. https://doi.org/10.1523/JNEUROSCI.0013-11.2011
3. Armstrong DL, Sauls CD, Goddard-Finegold J. Neuropathologic findings in short-term survivors of intraventricular hemorrhage. *Am J Dis Child*. 1987;141(6):617-621. https://doi.org/10.1001/archpedi.1987.04460060035027
4. Back SA. Perinatal white matter injury: the changing spectrum of pathology and emerging insights into pathogenetic mechanisms. *Ment Retard Dev Disabil Res Rev*. 2006;12(2):129-140. https://doi.org/10.1002/mrdd.20107
5. Mirzadeh Z, Merkle FT, Soriano-Navarro M, Garcia-Verdugo JM, Alvarez-Buylla A. Neural stem cells confer unique pinwheel architecture to the ventricular surface in neurogenic regions of the adult brain. *Cell Stem Cell*. 2008;3(3):265-278. https://doi.org/10.1016/j.stem.2008.07.004
6. Gensert JM, Goldman JE. Endogenous progenitors remyelinate demyelinated axons in the adult CNS. *Neuron*. 1997;19(1):197-203. https://doi.org/10.1016/s0896-6273(00)80359-1
7. Fancy SP, Zhao C, Franklin RJ. Increased expression of Nkx2.2 and Olig2 identifies reactive oligodendrocyte progenitor cells responding to demyelination in the adult CNS. *Mol Cell Neurosci*. 2004;27(3):247-254. https://doi.org/10.1016/j.mcn.2004.06.015
8. Nait-Oumesmar B, Decker L, Lachapelle F, et al. Progenitor cells of the adult mouse subventricular zone proliferate, migrate and differentiate into oligodendrocytes after demyelination. *Eur J Neurosci*. 1999;11(12):4357-4366. https://doi.org/10.1046/j.1460-9568.1999.00873.x
9. Picard-Riera N, Decker L, Delarasse C, et al. Experimental autoimmune encephalomyelitis mobilizes neural progenitors from the subventricular zone to undergo oligodendrogenesis in adult mice. *Proc Natl Acad Sci U S A*. 2002;99(20):13211-13216. https://doi.org/10.1073/pnas.192314199
10. Menn B, Garcia-Verdugo JM, Yaschine C, et al. Origin of oligodendrocytes in the subventricular zone of the adult brain. *J Neurosci*. 2006;26(30):7907-7918. https://doi.org/10.1523/JNEUROSCI.1299-06.2006
11. Lehtinen MK, Walsh CA. Neurogenesis at the brain-cerebrospinal fluid interface. *Annu Rev Cell Dev Biol*. 2011;27:653-679. https://doi.org/10.1146/annurev-cellbio-092910-154026
12. Wolswijk G, Noble M. Cooperation between PDGF and FGF converts slowly dividing O-2Aadult progenitor cells to rapidly dividing cells with characteristics of O-2Aperinatal progenitor cells. *J Cell Biol*. 1992;118(4):889-900. https://doi.org/10.1083/jcb.118.4.889
13. Engel U, Wolswijk G. Oligodendrocyte-type-2 astrocyte (O-2A) progenitor cells derived from adult rat spinal cord: in vitro characteristics and response to PDGF, bFGF and NT-3. *Glia*. 1996;16(1):16-26. https://doi.org/10.1002/(SICI)1098-1136(199601)16:1<16::AID-GLIA3>3.0.CO;2-9
14. Shi J, Marinovich A, Barres BA. Purification and characterization of adult oligodendrocyte precursor cells from the rat optic nerve. *J Neurosci*. 1998;18(12):4627-4636. https://doi.org/10.1523/JNEUROSCI.18-12-04627.1998
15. McKinnon RD, Piras G, Ida JA Jr, Dubois-Dalcq M. A role for TGF-beta in oligodendrocyte differentiation. *J Cell Biol*. 1993;121(6):1397-1407. https://doi.org/10.1083/jcb.121.6.1397
16. McKinnon RD, Smith C, Behar T, Smith T, Dubois-Dalcq M. Distinct effects of bFGF and PDGF on oligodendrocyte progenitor cells. *Glia*. 1993;7(3):245-254. https://doi.org/10.1002/glia.440070308
17. Diemel LT, Jackson SJ, Cuzner ML. Role for TGF-beta1, FGF-2 and PDGF-AA in a myelination of CNS aggregate cultures enriched with macrophages. *J Neurosci Res*. 2003;74(6):858-867. https://doi.org/10.1002/jnr.10837
18. Hinks GL, Franklin RJ. Distinctive patterns of PDGF-A, FGF-2, IGF-I, and TGF-beta1 gene expression during remyelination of experimentally-induced spinal cord demyelination. *Mol Cell Neurosci*. 1999;14(2):153-168. https://doi.org/10.1006/mcne.1999.0771
19. Frederick TJ, Wood TL. IGF-I and FGF-2 coordinately enhance cyclin D1 and cyclin E-cdk2 association and activity to promote G1 progression in oligodendrocyte progenitor cells. *Mol Cell Neurosci*. 2004;25(3):480-492. https://doi.org/10.1016/j.mcn.2003.11.015
20. Jiang F, Frederick TJ, Wood TL. IGF-I synergizes with FGF-2 to stimulate oligodendrocyte progenitor entry into the cell cycle. *Dev Biol*. 2001;232(2):414-423. https://doi.org/10.1006/dbio.2001.0208
21. Bansal R, Kumar M, Murray K, Morrison RS, Pfeiffer SE. Regulation of FGF receptors in the oligodendrocyte lineage. *Mol Cell Neurosci*. 1996;7(4):263-275. https://doi.org/10.1006/mcne.1996.0020
22. Bansal R, Kumar M, Murray K, Pfeiffer SE. Developmental and FGF-2-mediated regulation of syndecans (1-4) and glypican in oligodendrocytes. *Mol Cell Neurosci*. 1996;7(4):276-288. https://doi.org/10.1006/mcne.1996.0021
23. Sulaiman W, Nguyen DH. Transforming growth factor beta 1, a cytokine with regenerative functions. *Neural Regen Res*. 2016;11(10):1549-1552. https://doi.org/10.4103/1673-5374.193223
24. Bansal R, Marin-Husstege M, Bryant M, Casaccia-Bonnefil P. S-phase entry of oligodendrocyte lineage cells is associated with increased levels of p21Cip1. *J Neurosci Res*. 2005;80(3):360-368. https://doi.org/10.1002/jnr.20454
25. Palazuelos J, Klingener M, Aguirre A. TGFbeta signaling regulates the timing of CNS myelination by modulating oligodendrocyte progenitor cell cycle exit through SMAD3/4/FoxO1/Sp1. *J Neurosci*. 2014;34(23):7917-7930. https://doi.org/10.1523/JNEUROSCI.0363-14.2014
26. Casaccia-Bonnefil P, Tikoo R, Kiyokawa H, et al. Oligodendrocyte precursor differentiation is perturbed in the absence of the cyclin-dependent kinase inhibitor p27Kip1. *Genes Dev*. 1997;11(18):2335-2346. https://doi.org/10.1101/gad.11.18.2335
27. Casaccia-Bonnefil P, Hardy RJ, Teng KK, et al. Loss of p27Kip1 function results in increased proliferative capacity of oligodendrocyte progenitors but unaltered timing of differentiation. *Development*. 1999;126(18):4027-4037. https://doi.org/10.1242/dev.126.18.4027
28. Durand B, Fero ML, Roberts JM, Raff MC. p27Kip1 alters the response of cells to mitogen and is part of a cell-intrinsic timer that arrests the cell cycle and initiates differentiation. *Curr Biol*. 1998;8(8):431-440. https://doi.org/10.1016/s0960-9822(98)70177-0
29. Liao Y, Cotten M, Tan S, Kurtzberg J, Cairo MS. Rescuing the neonatal brain from hypoxic injury with autologous cord blood. *Bone Marrow Transplant*. 2013;48(7):890-900. https://doi.org/10.1038/bmt.2012.169

30. Liao Y, Geyer MB, Yang AJ, Cairo MS. Cord blood transplantation and stem cell regenerative potential. *Exp Hematol*. 2011;39(4):393-412. https://doi.org/10.1016/j.exphem.2011.01.002
31. Balseanu AT, Buga AM, Catalin B, et al. Multimodal approaches for regenerative stroke therapies: combination of granulocyte colony-stimulating factor with bone marrow mesenchymal stem cells is not superior to g-csf alone. *Front Aging Neurosci*. 2014;6:130. https://doi.org/10.3389/fnagi.2014.00130
32. Buga AM, Scheibe J, Moller K, et al. Granulocyte colony-stimulating factor and bone marrow mononuclear cells for stroke treatment in the aged brain. *Curr Neurovasc Res*. 2015;12(2):155-162. https://doi.org/10.2174/1567202612666150311112550
33. Drobyshevsky A, Cotten CM, Shi Z, et al. Human umbilical cord blood cells ameliorate motor deficits in rabbits in a cerebral palsy model. *Dev Neurosci*. 2015;37(4-5):349-362. https://doi.org/10.1159/000374107
34. Kluth SM, Radke TF, Kogler G. Increased haematopoietic supportive function of USSC from umbilical cord blood compared to CB MSC and possible role of DLK-1. *Stem Cells Int*. 2013;2013:985285. https://doi.org/10.1155/2013/985285
35. Schira J, Falkenberg H, Hendricks M, et al. Characterization of regenerative phenotype of unrestricted somatic stem cells (USSC) from human umbilical cord blood (hUCB) by functional secretome analysis. *Mol Cell Proteomics*. 2015;14(10):2630-2643. https://doi.org/10.1074/mcp.M115.049312
36. Kogler G, Radke TF, Lefort A, et al. Cytokine production and hematopoiesis supporting activity of cord blood-derived unrestricted somatic stem cells. *Exp Hematol*. 2005;33(5):573-583. https://doi.org/10.1016/j.exphem.2005.01.012
37. Coenen M, Kogler G, Wernet P, Brüstle O. Transplantation of human umbilical cord blood-derived adherent progenitors into the developing rodent brain. *J Neuropathol Exp Neurol*. 2005;64(8):681-688. https://doi.org/10.1097/01.jnen.0000173892.24800.03
38. Vinukonda G, Liao Y, Hu F, et al. Human cord blood-derived unrestricted somatic stem cell infusion improves neurobehavioral outcome in a rabbit model of intraventricular hemorrhage. *Stem Cells Transl Med*. 2019;8(11):1157-1169. https://doi.org/10.1002/sctm.19-0082
39. Purohit D, Finkel DA, Malfa A, et al. Human cord blood derived unrestricted somatic stem cells restore aquaporin channel expression, reduce inflammation and inhibit the development of hydrocephalus after experimentally induced perinatal intraventricular hemorrhage. *Front Cell Neurosci*. 2021;15:633185. https://doi.org/10.3389/fncel.2021.633185
40. Schira J, Gasis M, Estrada V, et al. Significant clinical, neuropathological and behavioural recovery from acute spinal cord trauma by transplantation of a well-defined somatic stem cell from human umbilical cord blood. *Brain*. 2012;135(Pt 2):431-446. https://doi.org/10.1093/brain/awr222
41. Kogler G, Sensken S, Airey JA, et al. A new human somatic stem cell from placental cord blood with intrinsic pluripotent differentiation potential. *J Exp Med*. 2004;200(2):123-135. https://doi.org/10.1084/jem.20040440
42. Liao Y, Itoh M, Yang A, et al. Human cord blood-derived unrestricted somatic stem cells promote wound healing and have therapeutic potential for patients with recessive dystrophic epidermolysis bullosa. *Cell Transplant*. 2014;23(3):303-317. https://doi.org/10.3727/096368913X663569
43. Georgiadis P, Xu H, Chua C, et al. Characterization of acute brain injuries and neurobehavioral profiles in a rabbit model of germinal matrix hemorrhage. *Stroke*. 2008;39(12):3378-3388. https://doi.org/10.1161/STROKEAHA.107.510883
44. Vinukonda G, Csiszar A, Hu F, et al. Neuroprotection in a rabbit model of intraventricular haemorrhage by cyclooxygenase-2, prostanoid receptor-1 or tumour necrosis factor-alpha inhibition. *Brain*. 2010;133(Pt 8):2264-2280. https://doi.org/10.1093/brain/awq107
45. Dohare P, Zia MT, Ahmed E, et al. AMPA-kainate receptor inhibition promotes neurologic recovery in premature rabbits with intraventricular hemorrhage. *J Neurosci*. 2016;36(11):3363-3377. https://doi.org/10.1523/JNEUROSCI.4329-15.2016
46. Kim MO, Kim SH, Cho YY, et al. ERK1 and ERK2 regulate embryonic stem cell self-renewal through phosphorylation of Klf4. *Nat Struct Mol Biol*. 2012;19(3):283-290. https://doi.org/10.1038/nsmb.2217
47. Hatzistergos KE, Quevedo H, Oskouei BN, et al. Bone marrow mesenchymal stem cells stimulate cardiac stem cell proliferation and differentiation. *Circ Res*. 2010;107(7):913-922. https://doi.org/10.1161/CIRCRESAHA.110.222703
48. Ko HR, Ahn SY, Chang YS, et al. Human UCB-MSCs treatment upon intraventricular hemorrhage contributes to attenuate hippocampal neuron loss and circuit damage through BDNF-CREB signaling. *Stem Cell Res Ther*. 2018;9(1):326. https://doi.org/10.1186/s13287-018-1052-5
49. Vinukonda G, La Gamma EF. Emerging therapies for brain recovery after IVH in neonates: cord blood derived mesenchymal stem cells (MSC) and unrestricted somatic stem cells (USSC). *Semin Perinatol*. 2022;46(5):151598. https://doi.org/10.1016/j.semperi.2022.151598
50. Hwang DH, Kim BG, Kim EJ, et al. Transplantation of human neural stem cells transduced with Olig2 transcription factor improves locomotor recovery and enhances myelination in the white matter of rat spinal cord following contusive injury. *BMC Neurosci*. 2009;10:117. https://doi.org/10.1186/1471-2202-10-117
51. Gomes FC, Sousa Vde O, Romao L. Emerging roles for TGF-beta1 in nervous system development. *Int J Dev Neurosci*. 2005;23(5):413-424. https://doi.org/10.1016/j.ijdevneu.2005.04.001
52. Farreny MA, Agius E, Bel-Vialar S, et al. FGF signaling controls Shh-dependent oligodendroglial fate specification in the ventral spinal cord. *Neural Dev*. 2018;13(1):3. https://doi.org/10.1186/s13064-018-0100-2
53. Laouarem Y, Traiffort E. Developmental and repairing production of myelin: the role of hedgehog signaling. *Front Cell Neurosci*. 2018;12:305. https://doi.org/10.3389/fncel.2018.00305
54. Baker J, Liu JP, Robertson EJ, Efstratiadis A. Role of insulin-like growth factors in embryonic and postnatal growth. *Cell*. 1993;75(1):73-82.
55. Mukai T, Mori Y, Shimazu T, et al. Intravenous injection of umbilical cord-derived mesenchymal stromal cells attenuates reactive gliosis and hypomyelination in a neonatal intraventricular hemorrhage model. *Neuroscience*. 2017;355:175-187. https://doi.org/10.1016/j.neuroscience.2017.05.006